

Features of hydrogenated amorphous silicon films developed under an unexplored region of parameter space of radio-frequency plasma-enhanced chemical vapor deposition

Sukti Hazra^{a)} and A. R. Middy^{b)}

Energy Research Unit, Indian Association for the Cultivation of Science, Jadavpur, Calcutta-700 032, India

C. Longeaud

Laboratoire de Génie Electrique de Paris, Ecole Supérieure d'Electricité, Universités Paris VI et Paris XI, Plateau de Moulon, 91192 Gif-Sur-Yvette Cedex, France

Swati Ray

Energy Research Unit, Indian Association for the Cultivation of Science, Jadavpur, Calcutta-700 032, India

(Received 7 September 1999; accepted for publication 25 February 2000)

Searching to improve stability of electronic properties under intense light illumination, hydrogenated amorphous silicon (*a*-Si:H) films have been fabricated by radio-frequency plasma-enhanced chemical vapor deposition with helium dilution of silane. The deposition conditions which correspond to the transition between the α regime and the powder regime have not been explored properly yet. The resulting materials show many new features: hydrogen bonding mostly monohydride, lower bonded hydrogen content, compact structure, higher efficiency-mobility-lifetime product ($\eta\mu\tau$) and density of states (DOS) above Fermi level lower than the reported values of the state-of-the-art *a*-Si:H films. The saturation time under light-soaking (AM 1) is fast (within 20 h) and the saturated value of $\eta\mu\tau$ and the DOS above the Fermi level is comparable to that of annealed state standard *a*-Si:H films. © 2000 American Institute of Physics. [S0003-6951(00)00517-9]

In an endeavor to develop stable hydrogenated amorphous silicon (*a*-Si:H) solar cells at low cost, there has been a great deal of research over the last twenty years to develop *a*-Si:H thin films having low defect density at annealed state. As a result of extensive scanning of deposition parameters space of a commonly used technique, the radio-frequency powered plasma-enhanced chemical vapor deposition (rf PECVD), and subsequent modeling of growth kinetics, a general agreement has emerged that low rf power and chamber pressure, the so-called α regime of PECVD, and hydrogen dilution of silane, are conducive to the growth of the state-of-art *a*-Si:H.¹ Other extreme of parameter space, high power and pressure, i.e., the γ regime, has been so far avoided, although the deposition rate could be increased, because of the onset of powder formation which eventually lead to the deterioration of film quality. However, there has been a growing consensus that the modification of hydrogen bonding and Si-Si network of *a*-Si:H films is the key to improve the stability of *a*-Si:H films which is of the utmost priority of the present day *a*-Si technology.² The growth of more stable *a*-Si:H of hot wire CVD compared to that of PECVD is a good demonstration for the above-mentioned approach.³ In order to explore the network structure of *a*-Si:H materials having better stability, we ventured into yet unexplored regime of parameter space close to powder regime and used helium (He) dilution of silane. Present authors

have already demonstrated that compared to hydrogen, He dilution of source gases is found to be more efficient for the improvement of microstructure of more complicated amorphous silicon germanium (*a*-SiGe:H) alloys.⁴⁻⁶ In this study, we report on new features of the electronic properties, density of state (DOS), and stability of *a*-Si:H films deposited close to the γ regime of rf PECVD.

The samples of this study have been deposited from a gas mixture of silane and helium, the total gas flow being maintained at 42.5 sccm, in a capacitively coupled rf powered (13.56 MHz) PECVD system. During film deposition, substrate temperature and rf power have been kept at 210 °C and 15 mW/cm², respectively, whereas chamber pressure has been varied from 0.5 to 2.2 Torr. Many measurements have been performed on these samples to confirm the consistency of the observations. The microstructure of the films have been analyzed by infrared vibrational spectroscopy [Fourier-transform infrared (FTIR)], Raman spectroscopy, small-angle x-ray scattering (SAXS), UV-VIS ellipsometry, and x-ray diffraction. The efficiency-mobility-lifetime products ($\eta\mu\tau$) of electrons have been measured under band-gap light with a generation rate of $3 \times 10^{18} \text{ cm}^{-3} \text{ s}^{-1}$. The DOS of these films has been investigated by complementary techniques like electron spin resonance (ESR), constant photocurrent method (CPM), and modulated photocurrent experiment (MPC). The light-soaking kinetics under various conditions of light and temperature have also been investigated.

The variations of the deposition rate (R_D) and bonded hydrogen contents (C_H) with chamber pressure (P_r) during deposition are shown in Fig. 1. The drastic increase of R_D of

^{a)}Present address: Electron Devices Division, Electrotechnical Laboratory, I-1-4 Umezono, Tsukuba, Ibaraki 305 8568, Japan; electronic mail: shazra@etl.go.jp

^{b)}Present address: SOLAREX, Newtown, Pennsylvania 18940.

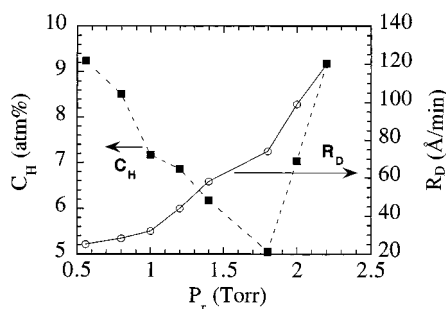


FIG. 1. Evolution of the deposition rate R_D and hydrogen content C_H with chamber pressure P_r .

the films for $P_r > 1.0$ Torr clearly indicates the transition of the rf discharge regime from the α regime, where electrons are accelerated by the oscillating plasma sheath edges (wave-riding or sheath heating mechanism) to the γ' regime (to distinguish from γ regime which is usually observed in He and Ar plasma due to secondary electron emission) where the dominant power dissipation mechanism is the Joule heating of the electrons of the bulk plasma. In the γ' regime, under high pressure, negatively charged powders start forming and are confined in the electric field developed within the sheaths which leads to better coupling of the rf power into the plasma.¹ Consequently, more electron impact dissociation of SiH_4 molecules in the sheaths occurs and hence, R_D increases for $P_r > 1.0$ Torr. It should be noted that the pressure is a crucial parameter and a good reproducibility of the sample properties is obtained only with a proper control of this parameter. Though the deposition occurs in a parameter region close to powder regime in which formation of crystalline silicon particles occurs, x-ray diffraction exhibits the usual broad peak typical of $a\text{-Si:H}$ showing no sign of crystalline component in the layers. The amorphous state of the material is also confirmed using UV-VIS ellipsometry, for which the spectra do not exhibit any peak at 4.2 eV. However, best fittings of the ellipsometry spectra are obtained accounting for a small amount of a crystalline phase ($<20\%$). Moreover, during Raman measurement, it is noted that with small application of laser power, the amorphous to nano/microcrystalline phase transformation occurs. This implies that the Si-Si network of these films is perhaps close to that of microcrystalline state. The dominant hydrogen bonding configuration is monohydride as observed by stretching vibrational spectra of Si-H bonds, however, the peak position is slightly shifted from 2000 to 2010 cm^{-1} .⁷ The absorption due to di/polyhydride component systematically decreases with the chamber pressure up to 1.8 Torr. Two overlapping peaks at 620 and 610 cm^{-1} corresponds to Si-H_n ($n=1,2,3$) wagging mode are observed. The bonded hydrogen content, as estimated by integrating the absorption peak around 620 cm^{-1} (infrared spectroscopy),⁸ decreases from 8 at % to around 5 at %, a quantity much lower than one usually finds in standard $a\text{-Si:H}$. Consistent with this observation the microvoid fraction in these films as estimated by SAXS is quite low ($<0.01\%$) and density (2.23 ± 0.01 gm/cc) is high compared to standard $a\text{-Si:H}$ films.⁹

Figure 2 shows the variation of efficiency-mobility-lifetime ($\eta\mu\tau$), dark conductivity (σ_d), and photosensitivity of the films with P_r . The values of $\mu\tau$ increase from 2

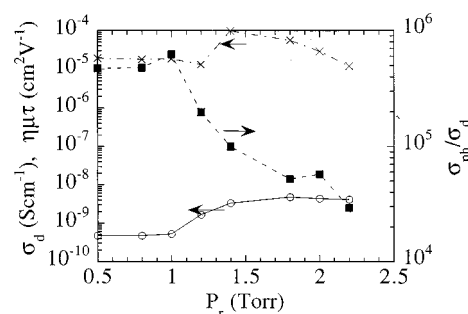


FIG. 2. Evolution of dark conductivity σ_d (\circ), mobility-lifetime product $\eta\mu\tau$ (\times), and photosensitivity σ_{ph}/σ_d with chamber pressure P_r .

$\times 10^{-5}$ to $9 \times 10^{-5} \text{ cm}^2 \text{ V}^{-1}$ accompanied by an increase of σ_d for $P_r > 1.0$ Torr. The variations of $\eta\mu\tau$ with P_r show that the best samples are obtained for pressure ranging from 1.4 to 1.8 Torr. It should be noted that the values of $\eta\mu\tau$ of the samples reported here are much higher than those reported in the literature for the state-of-the-art $a\text{-Si:H}$ films. The high values of $\eta\mu\tau$ cannot be attributed neither to any kind of n -type autodoping since the Fermi level positions (as measured from dark conductivity activation energy) of these samples vary between 0.70 and 0.90 eV, nor it can be explained from dangling bond density measured by conventional techniques. Indeed, the measurement of the DOS by ESR and CPM shows that the valence band tail widths and the deep defect density under the Fermi level of these samples are comparable to that of the state-of-the-art samples. We present in Fig. 3 the variations of dark and photoconductivity with temperature of two samples deposited with a pressure equal to 1.4 and 2 Torr, respectively. The activation energy of dark conductivity is 0.75 ± 0.05 eV for both samples, whereas the photoconductivity of sample deposited with 2 Torr behaves as that of a state-of-the-art $a\text{-Si:H}$ layer,¹⁰ the photoconductivity of sample deposited with 1.4 Torr is roughly continuously decreasing with temperature, exhibiting two unusual bumps. In both cases, photoconductivity has been measured under the same generation rate (F_{dc}), $7 \times 10^{13} \text{ cm}^{-2} \text{ s}^{-1}$. This is a clear signature that the DOS of this sample is different from that of typical $a\text{-Si:H}$ samples, a difference that may not be identified by means of ESR and CPM experiments.

Figure 4 shows the DOS measured from the MPC technique applied to a set of samples deposited under different chamber pressures. They are compared to the DOS obtained on a state-of-the-art $a\text{-Si:H}$ layer.¹⁰ The MPC technique is

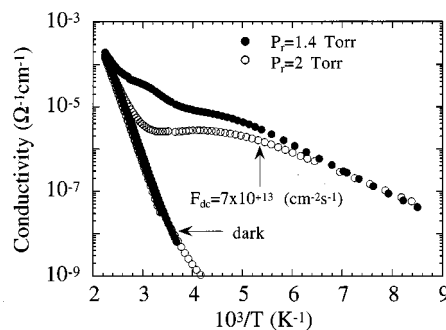


FIG. 3. Arrhenius plot of dark conductivity and photoconductivity for two samples deposited at 1.4 and 2 Torr, respectively.

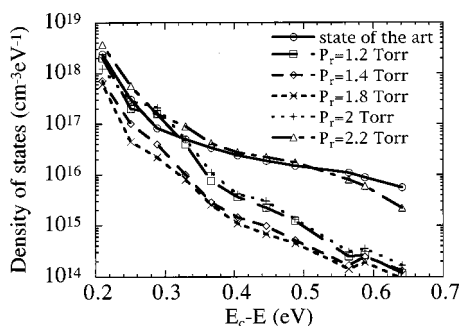


FIG. 4. DOS of a set of samples deposited under different chamber pressure measured from the MPC technique and compared to that of the state-of-the-art *a*-Si:H.

particularly suitable for the study of the DOS above the Fermi level. It is performed by varying the frequency of the excitation from 12 Hz to 40 kHz at a given temperature. The temperature is also varied between 150 and 450 K.¹¹ However, for the sake of clarity, we present in Fig. 4 only one point at a frequency of 3 kHz for one temperature. A direct link can be done between the deep defect density above the Fermi level and the values of the mobility-lifetime product: the lower the deep defect density, the higher the $\mu\tau$ product. Indeed, it should be noted that, although the conduction band tail is not modified a lot from one sample to another, for our best samples, the deep defect density, around 0.5 eV below the conduction band, is approximately 50 times lower than that of state-of-the-art *a*-Si:H. Thus, we expect that the high values of $\mu\tau$ are related to an increase of the lifetime instead of an increase of the mobility.

Figure 5 shows the variations of $\eta\mu\tau$ vs soaking time under white light (100 mW/cm²) at room temperature. Unlike commonly observed variations of $\eta\mu\tau$ in standard samples, the $\eta\mu\tau$ values saturate within short time (<20 h) and saturated values are still high and comparable to that of standard annealed *a*-Si:H films. Consistent with the change of $\mu\tau$ products, the Fermi level position of the samples, as measured from activation energy, moved deeper in the gap by approximately 150 meV after saturation. To ensure that the observed saturation is not related to surface effects, light-soaking experiments were also performed under volume ab-

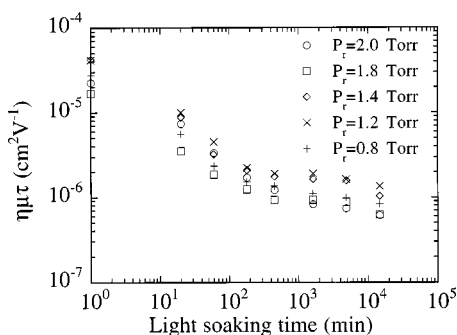


FIG. 5. Light-soaking kinetics of a set of samples prepared under different chamber pressure.

sorbed light ($\lambda > 650$ nm) at room and at high temperature (85 °C) with an illumination flux of 400 mW/cm². In both cases, the saturation of normalized photoconductivity occurs in a time much shorter than that of standard samples: 10 h at room temperature and 20 min at 85 °C to be compared to a few days and around 30 h respectively for a state-of-the-art sample.¹⁰ Thus, it seems that metastability of the samples is a bulk related effect and that its kinetics of degradation is completely different from that of typical *a*-Si:H samples. By means of the MPC experiment, the DOS of an annealed and light-soaked standard sample was compared to the DOS of one of our samples deposited at a total pressure of 1.8 Torr.¹⁰ The major conclusion from this study is that, in the light-soaked state, the deep defect density of our light-soaked sample is comparable to that of the annealed state-of-the-art sample.

The features in the transport behaviors and light-soaking kinetics described above could be linked to the microstructure and Si-Si bonding of these materials. Indeed, according to the results of FTIR, ellipsometry, and Raman experiments, the network structure of these materials seems to be close to or easily transformed into nano or microcrystalline phase. This result is another evidence that there is still a lot of room to improve the quality of *a*-Si:H films by controlling Si-H bonding and Si-Si network as also observed in case of films deposited by hot wire CVD, remote plasma PECVD, and chemical annealing.

In conclusion, *a*-Si:H films having characteristics, have been developed exploiting unexplored region of parameter space. These materials show high normalized photoconductivity and photosensitivity which are found to be consistent with their low deep defect density above the Fermi level. The saturation time under light soaking is fast (within 20 h) and saturated normalized photoconductivity and DOS above the Fermi level is comparable to that of annealed state-of-the-art *a*-Si:H. These facts, high $\eta\mu\tau$ and unusual variation with temperature, low DOS above the Fermi level, and fast degrading kinetics, reveal that these materials are different from state-of-the-art *a*-Si:H. The characteristics of these samples may be linked to its low microstructural defects and different Si-Si network.

¹J. Perrin, in *Plasma Deposition of Amorphous-based Materials*, edited by G. Bruno, P. Capezzuto, and A. Madan (Academic, New York, 1995), pp. 216–218.

²S. Guha, J. Non-Cryst. Solids **198–200**, 1076 (1996).

³A. H. Mahan, B. P. Nelson, S. Solomon, and R. S. Crandall, J. Non-Cryst. Solids **137 & 138**, 657 (1991).

⁴A. R. Middy, S. Hazra, and S. Ray, J. Appl. Phys. **76**, 7578 (1994).

⁵S. Hazra, A. R. Middy, J. K. Rath, S. Basak, and S. Ray, Jpn. J. Appl. Phys., Part 1 **34**, 5956 (1995).

⁶A. R. Middy, S. C. De, and S. Ray, J. Appl. Phys. **73**, 4622 (1993).

⁷S. Hazra and S. Ray, Solid State Commun. **105**, 755 (1998).

⁸H. Shanks, J. C. Fang, L. Ley, M. Cardona, F. J. Demond, and S. Kalbitzer, Phys. Status Solidi B **100**, 43 (1980).

⁹D. L. Williamson (private communication).

¹⁰A. R. Middy, S. Hazra, S. Ray, A. K. Barua, and C. Longeaud, J. Non-Cryst. Solids **198–200**, 1067 (1996).

¹¹J. P. Kleider and C. Longeaud, Solid State Phenom. **44–46**, 597 (1995).